EPJ Web of Conferences **66**, 02105 (2014)
DOI: 10.1051/epjconf/ 20146602105

Study of nuclei around $Z = 28$ by large-scale shell model calculations

Yusuke Tsunoda[1,a], Takaharu Otsuka[1,2,3], Noritaka Shimizu[2], Michio Honma[4], and Yutaka Utsuno[5]

[1]*Department of Physics, University of Tokyo, Tokyo 113-0033, Japan*
[2]*Center for Nuclear Study, University of Tokyo, Tokyo 113-0033, Japan*
[3]*National Superconducting Cyclotron Laboratory, Michigan State University, East Lansing, Michigan, USA*
[4]*Center for Mathematical Sciences, University of Aizu, Ikki-machi, Aizu-Wakamatsu, Fukushima 965-8580, Japan*
[5]*Advanced Science Research Center, Japan Atomic Energy Agency, Tokai, Ibaraki, 319-1195, Japan*

Abstract. We study Cr and Ni isotopes by using Monte Carlo shell model (MCSM) calculations in a pfg_9d_5 model space. In the MCSM, a wave function is represented as a linear combination of angular-momentum- and parity-projected deformed Slater determinants (MCSM bases) and we can obtain eigenstates in a large model space such as pfg_9d_5 space. We study intrinsic shapes of nuclei by using deformations of MCSM bases before projection. We show results of MCSM calculations in Cr and Ni isotopes and a level scheme of ^{68}Ni and discuss the magicity of $N = 40$ in Cr and Ni isotopes and shape coexistence in ^{68}Ni.

1 Introduction

An exotic nucleus is a nucleus whose neutron number is much larger or smaller than its proton number and shows various phenomena such as the shell evolution. The exotic nucleus has different shell structure from that of ordinary nucleus and can show different magic numbers. We use a pfg_9d_5 model space, which consists of the $0f1p$ shell, $0g_{9/2}$ and $1d_{5/2}$ orbits, in order to treat magic numbers 28, 50 and a submagic number 40. Conventional shell-model calculations are difficult in this large model space and we use the Monte Carlo shell model (MCSM) [1]. We discuss the strength of the magicity of $N = 40$ in Cr ($Z = 24$) and Ni ($Z = 28$) isotopes and shape coexistence in a doubly magic nucleus ^{68}Ni.

2 Monte Carlo Shell Model

We diagonalize a Hamiltonian matrix in a model space and obtain eigenstates in shell-model calculations. We can perform direct diagonalization in a model space where *m*-scheme dimension is about 10^{11} at most. However, the dimension is more than 10^{15} in the pfg_9d_5 space. In the MCSM, we diagonalize a Hamiltonian matrix in a small subspace spanned by a small number (around 100) of

[a]e-mail: ytsunoda@nt.phys.s.u-tokyo.ac.jp

angular-momentum- and parity-projected deformed Slater determinants (MCSM bases), and eigenstates are approximated by linear combinations of MCSM bases. The MCSM wave function $|\Psi_N\rangle$ is given as

$$|\Psi_N\rangle = \sum_{n=1}^{N} \sum_{K=-J}^{J} f_{n,K}^{(N)} P_{MK}^{J\pi} |\psi_n\rangle, \qquad |\psi_n\rangle = \prod_k \left(\sum_l D_{lk}^{(n)} c_l^\dagger \right) |-\rangle, \tag{1}$$

where $|\psi_n\rangle$ is a Slater determinant, $P_{MK}^{J\pi}$ is the angular-momentum and parity projector, $c_l^\dagger$ is a creation operator, and $|-\rangle$ is an inert core. Coefficients $f_{n,K}^{(N)}$ are determined by diagonalizing Hamiltonian matrix in a subspace spanned by MCSM bases $P_{MK}^{J\pi}|\psi_n\rangle$. We perform angular-momentum and parity projection by using the numerical integration with about 50,000 mesh points. Calculations in each mesh point are performed parallelly with a supercomputer. Coefficients $D_{lk}^{(n)}$ in MCSM bases are determined to lower energy eigenvalues with a method based on the auxiliary-field Monte Carlo and the conjugate gradient method.

We use the extrapolation using the energy variance [2, 3] and calculate more accurate energy eigenvalues. We change the number of MCSM bases N and calculate the energy expectation value $\langle H \rangle$ and the energy variance $\langle \Delta H^2 \rangle = \langle H^2 \rangle - \langle H \rangle^2$ of the wave function $|\Psi_N\rangle$. As N increases, $\langle H \rangle$ and $\langle \Delta H^2 \rangle$ approach the exact energy and zero respectively. We fit $\langle H \rangle$ by a second polynomial of $\langle \Delta H^2 \rangle$ and extrapolate the energy to $\langle \Delta H^2 \rangle = 0$.

3 Effective Interaction

We use the effective interaction used in Ref. [4, Sec. 4]. Two-body matrix elements (TBMEs) of the interaction consist of three parts. TBMEs in the pf shell are those of the GXPF1A interaction [5] and TBMEs in the f_5pg_9 space related to the $0g_{9/2}$ orbit are those of the JUN45 interaction [6]. The GXPF1A and JUN45 interactions were determined by combining microscopically derived interactions with a minor empirical fit. The other TBMEs are from the G-matrix effective interaction [7] calculated with the chiral N3LO interaction [8]. The Coulomb interaction is not considered and the isospin symmetry is conserved. We made further corrections of single-particle energies and monopole interactions.

4 Results

We calculated 0^+ and 2^+ yrast states in Cr and Ni even-even isotopes systematically and calculated many spin-parity states of ^{68}Ni. We took 50 MCSM bases for Cr isotopes, 80 bases for Ni isotopes except ^{68}Ni 0^+ states, and 120 bases for ^{68}Ni 0^+ states. The contamination of the spurious center-of-mass motion is sufficiently suppressed by using the prescription of Gloeckner and Lawson [9] with $\frac{\beta_{\rm c.m.}}{A}\hbar\omega = 5$ MeV. We took effective charges as $(e_p, e_n) = (1.5, 0.5)e$.

Figure 1 shows excitation energies of 2^+ yrast states in Cr and Ni isotopes and MCSM results reproduce experimental values well. The high excitation energy at $N = 40$ in Ni isotopes suggests the magicity of $N = 40$. However, excitation energies in Cr isotopes are low around $N = 40$ and the magicity of $N = 40$ vanishes. Figure 2 shows $B(E2; 0_1^+ \to 2_1^+)$ transition probabilities in Cr and Ni isotopes. $B(E2)$ values around $N = 40$ are small in Ni isotopes and large in Cr isotopes, which also suggests the magicity of $N = 40$ in Ni isotopes and the missing magicity of $N = 40$ in Cr isotopes. This change of the magicity of $N = 40$ may be caused by the change of the $N = 40$ shell gap and the magicity of $Z = 28$ in Ni isotopes.

We cannot study the intrinsic deformations of 0^+ states directly in ordinary shell-model calculations because wave functions of 0^+ states are spherical. In the MCSM, we can study deformations of

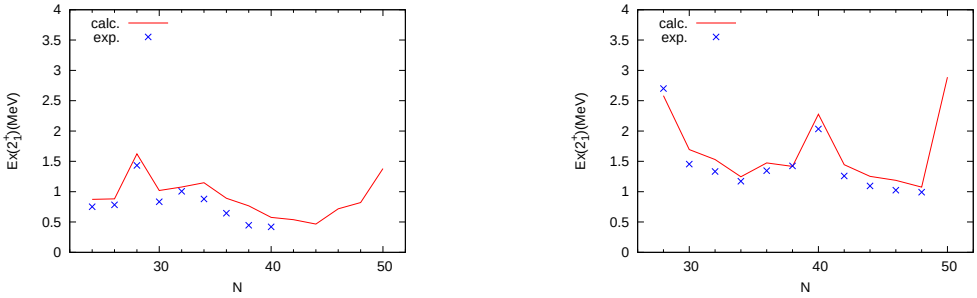

Figure 1. Excitation energies of 2_1^+ states in Cr (left) and Ni (right) isotopes. Experimental values are taken from Ref. [10].

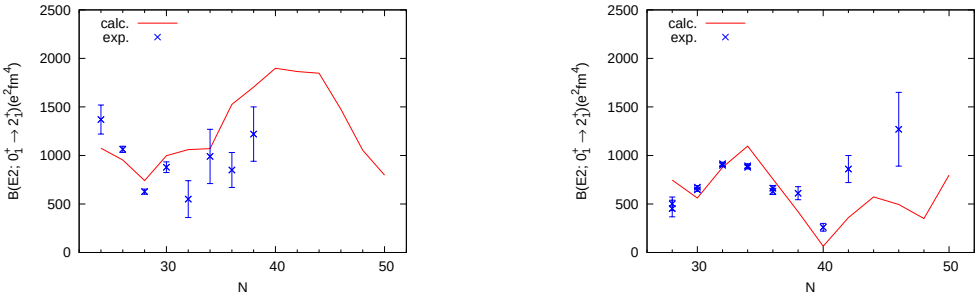

Figure 2. $B(E2; 0_1^+ \rightarrow 2_1^+)$ values in Cr (left) and Ni (right) isotopes. Experimental values are taken from Ref. [11].

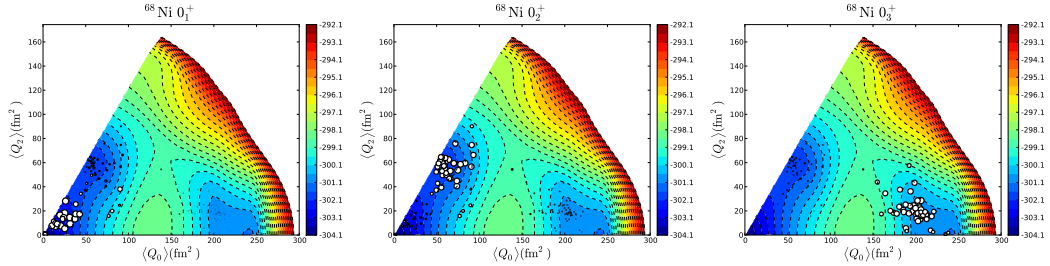

Figure 3. Total energy surfaces of $0^+_{1,2,3}$ states in ^{68}Ni. The positions of circles represent quadrupole deformations of unprojected MCSM bases. The areas of circles represent overlap probabilities between bases and the wave function.

0^+ states by using MCSM bases before angular-momentum projection. Figure 3 shows total energy surfaces of ^{68}Ni calculated with Q-constrained Hartree-Fock calculations [12]. There are three minimum points corresponding to spherical, oblate and prolate shapes on the total energy surface. Circles on the total energy surface correspond to MCSM bases and quadrupole deformations of the bases are calculated before projection. The areas of the circles represent overlap probabilities between bases and the wave function. Figure 3 shows that the 0_1^+, 0_2^+ and 0_3^+ states correspond to spherical, oblate and prolate shapes respectively.

Figure 4 shows the level scheme of ^{68}Ni. ^{68}Ni is an interesting nucleus because its proton number 28 is a magic number and its neutron number 40 is a submagic number. Our results reproduce experimental values including non-yrast and negative-parity states with slightly

high energies. Our analysis of deformations using unprojected bases shows that 0^+_1 state is spherical, 0^+_2, 2^+_1, 4^+_1 and 6^+_1 states are oblate, and 0^+_3, 2^+_2, 4^+_2 and 6^+_2 states are prolate. There are oblate and prolate rotational bands. The 8^+_1 state is oblate shape but indicates different properties from other oblate-deformed states. 6^+_1 and 8^+_1 states have close energies and the $B(E2; 8^+_1 \rightarrow 6^+_1)$ value is small. Highly deformed 0^+_3 and 2^+_2 states have been predicted by shell-model calculations in Ref. [14], but shapes of other states in their calculations are not reported.

5 Summary

We performed MCSM calculations of Cr and Ni isotopes in pfg_9d_5 space and studied nuclear intrinsic shapes by using deformations of unprojected MCSM bases. We showed the change of $N = 40$ magicity in Cr and Ni isotopes and three 0^+ states of ^{68}Ni with different shapes and close energies. The calculated excitation energies of ^{68}Ni reproduce experimental values including non-yrast and negative-parity states. These various properties were obtained from the same interaction and we are investigating other nuclei with this interaction.

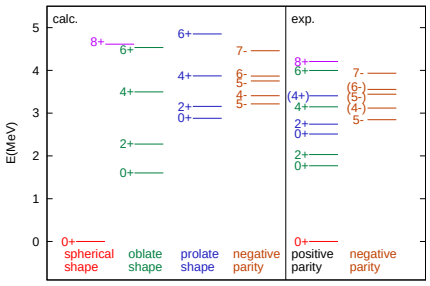

Figure 4. The level scheme of ^{68}Ni. Experimental values are taken from Ref. [13].

Acknowledgments

We thank Prof. M. Hjorth-Jensen for providing the G-matrix effective interaction. This work has been supported by Grant-in-Aid for JSPS Fellows (No. 258994) and HPCI Strategic Program field 5, MEXT, Japan. The numerical calculations were performed mainly on the K computer at the RIKEN AICS (Proposal number hp120284), the FX10 supercomputer at the University of Tokyo and the T2K Open Supercomputers at the University of Tokyo and the University of Tsukuba.

References

[1] T. Otsuka *et al.*, Prog. Part. Nucl. Phys. **47**, 319 (2001)
[2] N. Shimizu *et al.*, Phys. Rev. C **82**, 061305(R) (2010)
[3] N. Shimizu *et al.*, Phys. Rev. C **85**, 054301 (2012)
[4] N. Shimizu *et al.*, Prog. Theor. Exp. Phys. **2012**, 01A205 (2012)
[5] M. Honma *et al.*, Eur. Phys. J. A **25**, s01 499 (2005)
[6] M. Honma *et al.*, Phys. Rev. C **80**, 064323 (2009)
[7] M. Hjorth-Jensen *et al.*, Phys. Rep. **261**, 125 (1995)
[8] D. R. Entem *et al.*, Phys. Rev. C **68**, 041001(R) (2003)
[9] D. H. Gloeckner *et al.*, Phys. Lett. B **53**, 313 (1974)
[10] National Nuclear Data Center, information extracted from the NuDat 2 database, http://www.nndc.bnl.gov/nudat2/
[11] B. Pritychenko *et al.*, Atomic Data and Nuclear Data Tables **98**, 798 (2012)
[12] P. Ring and P. Schuck, *The Nuclear Many-Body Problem* (Springer-Verlag, New York, 1980)
[13] R. Broda *et al.*, Phys. Rev. C **86**, 064312 (2012)
[14] A. Dijon *et al.*, Phys. Rev. C **85**, 031301(R) (2012)